Cohesive crack growth modelling in heterogeneous materials

Jiří Vala and Vladislav Kozák

Abstract—Prediction of the crack growth of the brittle and quasi-brittle fracture of structural materials is studied. Crack extension is simulated by means of element extinction algorithms (cohesive elements respectively). The principal effort is concentrated on the application of the cohesive zone model with the various traction separation laws. Determination of micromechanical parameters is based on the combination of static tests, microscopic observation and numerical calibration procedures. The attention is paid on the influence of initial value of *J*-integral and the slope of *R*-curve which is modelled by the 3-dimensional finite element method. The practical applications refer to the modelling of the fracture behaviour of structural steels, intermetalic alloys and fibre composites.

Index Terms—Brittle fracture, cohesive crack growth, traction separation law, computational modelling.

I. INTRODUCTION

DEVELOPMENT and design of advanced equipments and components introduces the question how to ensure the operational security. Safety factors are connected with and dependent on the presence of the defects originated during production or service of the given part or components. An effort is concentrated on the description, eventually prediction of the fracture behaviour of bodies with a priori cracks or defects created during service loading.

Cohesive crack models are nowadays widely used to predict cracking processes in the materials. The importance of the cohesive zone approach is emphasized to analyze the localization and failure in engineering materials. The micromechanical modeling encounters a new problem that is different from assumption of continuum mechanics. The material is not uniform on the microscale, but a material element has its own complex microstructure and the concept of a representative volume element (RVE) has been introduced. The material separation and damage of the structure is described by the interface element. Using this technique, the behavior of the material is split into two parts: i) the damage of the free continuum with arbitrary material law and ii) the cohesive interface between the continuum elements.

From a variety of damage models, the cohesive models, derived in [1] and [2], seem to be especially perspective for practical applications. Thanks to their phenomenological character, they can be adapted for various kinds of materials and damages. Cohesive models or (more often) cohesive zone models (CZM) by [3] are used to simulate fracture and fragmentation processes in metallic, polymeric, ceramic materials and composites. Instead of an infinitely sharp crack envisaged in linear elastic fracture, the energy from the process zone is transferred from external work both in the forward and
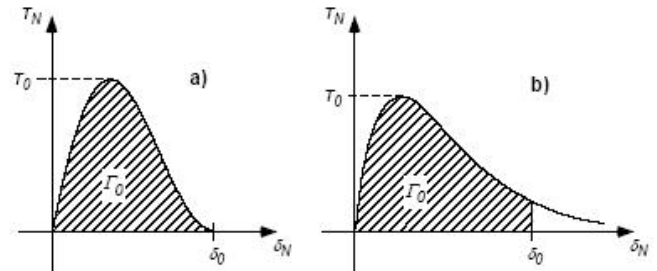

Fig. 1.   Examples of the traction-separation law.

wake regions of the expanding crack. Base principle of CZM is using cohesive elements for crack and damage modelling, while the classical continuum elements are undamaged. In terms of modelling, the separation of materials is realized using cohesive elements in the boundary line between classical elements of continuum. Using cohesive models, the behaviour of materials is considered using two types of elements: i) the former element for classical continuum, ii) the latter connecting cohesive element. The separation of such connecting cohesive elements is computed from the displacement of neighbouring continuum elements. Generally the separation is dependent on the normal and shear stresses.

In case of the cohesive models we need to identify the hypothetical crack tip to determine the crack driving force by using traction-separation models that are expressed in the shape of the T-δ curve. The maximum value of T has usually the character of cohesive strength; there is the physical crack tip where the separation has the maximum value at this distance, i.e. the crack is fully separated and the energy absorption for decohesion is total, as analyzed in [4]; for the illustration see two versions of the traction-separation law on Figure 1. The concept of the cohesive zone model has been widely employed to investigate various material failure phenomena; here we shall mention only some results important for our further considerations, whereas much more historical conjunctions including application scopes can be found in [5] and [6].

Since the analytic computational approaches give significant result only in very special cases, typically for the simulation of well-organized experiments, which is often valid also for semianalytic considerations, relying on classical infinite functions series and numerical quadrature, the majority of recent computational algorithms works with finite elements or similar techniques, namely with various implementations of the extended finite element method (XFEM) by [7] or [8], or with the cohesive segments method by [9], handling the

nucleation, growth and coalescence of multiple cracks. Some advantages of meshfree cohesive modelling of failure, namely of the reproducing kernel particle method (RKPM) within the framework of wavelet theory, are noticed in [10], together with the comparison of the cohesive zone approach and the atomistic view. The analysis of quasistatic brittle fracture in inhomogeneous media by [11] relies on the method of iterated conformal maps, distinguishing between fracture patterns in three basic modes. Really, there are three ways of applying a force to enable a crack to propagate: i) opening mode (tensile stress is normal to the plane of the crack), ii) sliding mode (shear stress acts parallel to the plane of the crack and perpendicular to the crack front) and iii) tearing mode (shear stress acts parallel to the plane of the crack and parallel to the crack front). The brittle-to-ductile transition (BDT), as well as the fracture toughness of semi-brittle materials, is studied the competition between the bond breaking at the crack tip and the mechanisms that govern crack tip plasticity at the atomic scale in [12]. The element-free Galerkin method (EFG), introduced in [13], substitutes the standard Galerkin finite element technique by the implementation of interface elements for the representation of displacement discontinuities due to cracks.

Limited accuracy of all crack growth predictions, depending on the creation of geometric singularities due to certain nonlocal constitutive relations, motivates the development of still alternative approaches, utilizing i) statistical considerations, ii) fractal theory, iii) advanced geometrical description of macro- and microfractured zones or iv) both physical and mathematical homogenization and scale-bridging. In the following remarks we shall try to preserve this classification, although some recent approaches cannot be assigned to just one of the classes i) – iv). Starting with i), whereas the Weibull function in [14] is introduced as simple mathematical relation that is capable of describing the variability in strength, [15] presents the complete Weibull fracture statistics of ceramics and [16] understands the brittle crack growth as the forced separation of chemically bonded surfaces, working with the survival probability within the separation zone. In ii) the generalization of [11] to fractal cracks, derived in [1], opens the way to the fractal-based mesoscopic analysis of damage and fracture in heterogeneous materials by [20], as well as to such discrete cohesive crack modelling by [21]; [22] then works with the fractal statistics of fragmentation (breaking a solid into separate fragments caused by multiple fractures) of brittle materials, supported by original experiments and signal processing techniques. From the point of view of iii) the most difficult problem is to complete the general nonlinear geometrical concept of [23] by the adequate physical considerations, including material characteristics identifiable in engineering practice, as documented by [24]. In iv) the RVE-based average approaches for a cohesive zone by [25] and [26] are still the most frequent; however, the exploitation of more advanced bridging between macro- and microscale models of cohesive fracture, as in [27], as well as of the formal mathematical homogenization like the Γ-convergence for rapidly oscillating functions in [28], should be noticed.

Regardless of quite different material structures, other size of specimens, particles in a matrix, etc., similar approaches are applied also to the composites utilized in civil engineering, as for the a masonry composite made of brick units and mortar arranged forming layers by [29] and in most applications for concrete. Some additional physical processes should not be neglected in this case: namely the cohesive damage friction interface model, suggested in [30], accounts for water pressure on crack propagation, whereas the semianalytic approach of [31] to reinforced cementitious composites is able to study the effects of fracture toughness, of crack bridging and of initial unbridged flaw size, thanks to the very special physical and geometric setting, due to the need of easy comparison with standard experimental results. The multi-scale approaches like [32] and fractal ones like [33] have been developped for concrete, too.

II. PHYSICAL AND MATHEMATICAL BACKGROUND

Let us introduce the basic physical and mathematical assumptions and notations of the cohesive zone approach, needed in this paper to understand (at certain minimal generality level) the crack behaviour of some material classes, important in engineering practice. A lot of potential improvements could be inspired by *Introduction*; however, the implementation of a general geometrical description of finite structured deformation, as well as of results from classical or fuzzy statistics, fractal theory or two-scale and similar types of convergences on homogenization structures would make this text very reader-unfriendly.

As a model problem, let us consider a domain Ω in the 3-dimensional Euclidean space R^3, occupied by a deformable body, supplied with the Cartesian coordinate system $x = (x_1, x_2, x_3)$; some (local, formally outward) unit normals $n = (n_1, n_2, n_3)$ are assumed to exist (almost) everywhere on the boundary $\partial\Omega$ of Ω in R^3. We shall study the behaviour of a deformable body on certain time interval I, starting from the zero time.

Let $u = (u_1, u_2, u_3)$ denote the displacement related to the above mentioned reference geometrical configuration; their zero-time initial values (compatible with Eq. 1, as formulated below) are prescribed. In the following considerations, i, j, k and l will be Einstein summation indices from the set $\{1, 2, 3\}$; if no comments are added, all relation will be valid for all values of free indices from this set. For simplicity, an index i preceded by a comma means a partial derivative with respect to x_i: e. g. $\psi_{j,i}$ can be used instead of the full notation $\partial\psi_j/\partial x_i$. Unlike such derivatives, an upper dot means a partial derivative with respect to any time t taken from I. the following equations should be then valid on I (without additional explanations).

Let us suppose that $\partial\Omega$ can be decomposed to its disjoint parts Γ, Θ and Ξ. We shall consider the Dirichlet boundary conditions

$$u_i = 0 \qquad \text{on } \Theta \qquad (1)$$

and the following loads: the volume ones $f = (f_1, f_2, f_3)$ on Ω and the surface ones $g = (g_1, g_2, g_3)$ on Γ. The knowledge of the material density ρ on Ω will be needed, too. The notation Ξ is reserved for the crack; its time development is possible.

For the stresses σ_{ij} the well-known Cauchy equilibrium condition reads

$$\sigma_{ij,j} + f_i = \rho \ddot{u}_i \qquad \text{on } \Omega, \qquad (2)$$

together with the Neumann boundary conditions

$$\sigma_{ij} n_j = g_i \qquad \text{on } \Gamma. \qquad (3)$$

Moreover, introducing the strains $\varepsilon_{kl}(u)$, for the small strain approximation identifiable with $(u_{k,l} + u_{l,k})/2$, we need some constitutive relations to obtain σ_{ij}, typically

$$\dot{\sigma}_{ij} = G_{ij}(\dot{\varepsilon}(u)) \qquad \text{on } \Omega \qquad (4)$$

with some prescribed mapping G_{ij} where ε can be considered as a symmetrical matrix of all $\varepsilon_{kl}(u)$, following [9], p. 72. In the simplest case the choice $G_{ij}(\varepsilon(u)) = C_{ijkl}\varepsilon_{kl}(u)$ leads to the Hooke law with constant characteristics C_{ijkl} (thus time derivatives can be removed) generating a symmetrical positive definite matrix (which still admits nonhomogeneous and anisotropic materials).

Up to now, at least with empty Ξ (which may be the initial case), we have only the standard problem of deformation of linear (or similar) elastic body. Let us moreover suppose that Ξ, representing a crack, consists of two identical parts Ξ^+ and Ξ^-, distinguished by the opposite orientation of n only. The value of u on the crack tip, because of the irregularity of such point, must be evaluated separately, using some J- or K-nonlocal stress integrals; this can lead to the irreversible enlargement of Ξ in time. Nevertheless, the 2-dimensional simplifications are utilized in most computational tools − cf. [7], p. 831.

The Neumann boundary condition analogous to Eq. 3 with 0 instead of g_i could be considered on Ξ outside the cohesive zone; To force the material nonpenetrability, for the notation $\delta u_i = u_i^+ - u_i^-$ where u_i^+ and u_i^- have to be understood in the sense of traces of u from Ω then we should check also $\delta u_i n_i \geq 0$ (which is rarely done in practical algorithms).

Inside the cohesive zone the physical considerations are more delicate: a new constitutive relation has to be introduced on Ξ (active on its part), e. g. in the form presented in [9], pp. 73 and 77,

$$\dot{\tau}_i = \gamma_i(\delta \dot{u}) \qquad \text{on } \Xi \qquad (5)$$

with some prescribed mapping γ_i where $\delta \dot{u}$ can be introduced in the similar way as δu and the discontinuity tractions τ_i replace g_i from Eq. 3. The most simple form of such relation seems to be $\dot{\tau}_i = \kappa \delta \dot{u}$ with certain tangent stiffness of the traction separation law. One can observe very special forms, as rectangular, (piecewise) linear, etc., of cohesive laws in engineering practice (cf. [7], p. 816); for more details see the following section and all relevant references.

Introducing the set of admissible displacements $\mathcal{V}$ as those displacement from appropriate function spaces satisfying Eq. 1 (Lebesgue, Sobolev, Bochner, etc. spaces are exploited in most cases to guarantee the formal correctness of all formulations and the existence and uniqueness of variational or weak solutions, at least for linear and selected semilinear problems),

applying the Green‑Ostrogradskiĭ theorem (on the integration by parts), we are able to convert (2) and (3) to

$$(\varepsilon_{ij}(v), \sigma_{ij}) - (v_i, \rho \ddot{u}_i) + \langle \delta v_i, \tau_i \rangle \qquad (6)$$
$$= (v_i, f_i) + \langle v_i, g_i \rangle \quad \forall\, v \in \mathcal{V};$$

here (ψ, ϕ) mean the integrals of $\psi(x)\phi(x)$ over Ω (with hidden Einstein sums), $\langle \psi, \phi \rangle$ and $\langle \psi, \phi \rangle_*$ then the similar integrals over Γ and Ξ_+, respectively. Both constititive relations Eq. 4 and Eq. 5 are supposed to be hidden in Eq. 6. Consequently some integral equation of the type Eq. 6, representing the Galerkin formulation of our model problem, is applied in most numerical algorithms based on (classical or extended) finite element techniques and occurs also in derivation of numerous meshless algorithms, both dynamic and quasistatic ones.

III. Crack behaviour of selected materials

A. Structural steels

The standard tensile experiments have been used to determine material curve for characterization of the elastoplastic behaviour of tested material. The relation σ_e - ϵ_e was found, but key problem is the validity of this relation after necking. According to many experimental observations in [5] the new approximate curve was received. For forged 42CrMo4 steel the ductile fracture was predicted and $J - \Delta a$ curve is calculated by cohesive elements using Warp3D and Abaqus codes.

For the determination of the cohesive stress, T_0 in the case of normal fracture (mode I) a set of twelve experiments for tensile notched bars was done. The mean value of the cohesive stress T0 was determined from the above mentioned set and from the computations for the material curve received from the waisted tensile specimens; T_0 is then 2000 MPa. For determination of the stress-strain distribution the standard FEM Abaqus package with CAX4 elements was used. The standard CT specimens were used for J-integral determination according the ASTM 1820-99a procedure (based on measurement of the $J - \Delta a$ curve). The experimentally determined value of J_i was found to be 115 MPa.mm. This value was calibrated using numerical procedure using WarpD.

The numerical modelling was realized with all material curves. The standard FEM package Abaqus has been utilized. Set of computations were applied to the calibration of the cohesive parameters used for $J - \Delta a$ curve prediction. Various combinations for T_0 and J_i were tested. In Figure 2 the values J_i are marked as Cohe_1, Cohe_2 and Cohe_3 (J_i with values 110, 120, 130) and received data were compared with the experimental values. The best correlation was found for first value of J_i=110 MPa.mm. From the above analyses follows the prime combination of the cohesive parameters (T_0=2000 MPa, J_i=110 MPa.mm).

Single three point bend specimen SE(B) has been used for experimental prediction of the $J - R$ curve. Using the cohesive parameters received on the notched specimens T_0 and J_i on the CT specimens the numerical simulation of the stable crack growth was done and $J - R$ curve was predicted – see Figure 3. The FE mesh consists from 8560 nodes and 7155 element C3D8 (Abaqus). Owing to numerical instability more than 1000 loading steps were applied.
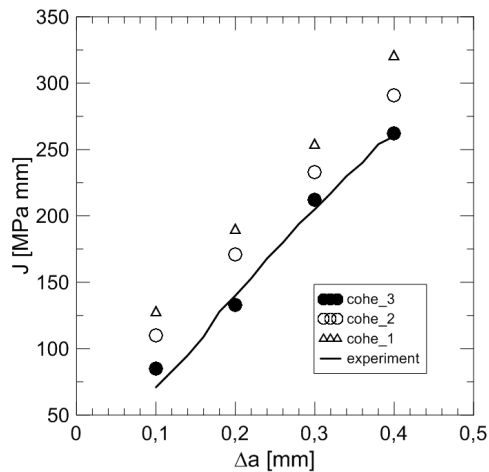
Fig. 2. J_i calibration on CT specimen.
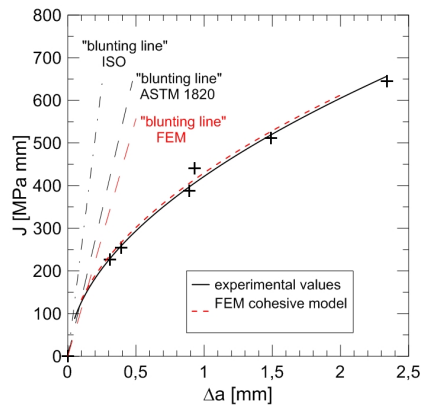
Fig. 3. $J-R$ curve for SE(B) specimen.

B. Intermetallic alloy TiAl

Main goal of the experimental work was the evaluation of the flexural strength tests in the temperature range from room temperature up to 800 C for the intermetallic alloy TiAl (see [36]). The materials used in this investigation had the composition Ti-48Al-2Cr-2Nb-1B and Ti-46Al-0,7Cr-0,1Si-7Nb-0,2Ni (marked I and F).
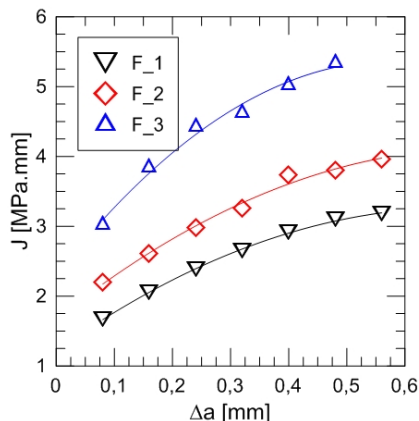
Fig. 4. $J-R$ curve: $K = 14$ MPa.m$^{1/2}$, $K = 16.3$ MPa.m$^{1/2}$, $K = 20$ MPa.m$^{1/2}$ (Chevron notch, $\sigma_y = 200$ MPa).
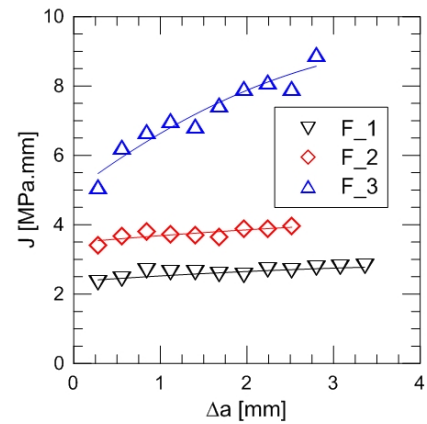
Fig. 5. $J-R$ curve: $K = 14$ MPa.m$^{1/2}$, $K = 16.3$ MPa.m$^{1/2}$, $K = 20$ MPa.m$^{1/2}$ (sharp notch, $\sigma_y = 200$ MPa).

The FEM mesh with two modifications was created for the stress analysis. The first one had 10000 C3D8 elements and second one 90000 elements. After some numerical test was found that there is a very small discrepancy between them and a mesh with smaller density of elements was used for next computations. The cohesive 3D elements COH3D8 with zero thickness were used for cohesive zone modelling using FEM packages Abaqus and Warp3D.

The input parameters of the cohesive model with linear damage development for alloy I were determined following experiments for fracture toughness. In this way the fracture energy was assigned expressing the area below the TSL. Parameter T_0 was evaluated from the values of fracture stresses. The value δ_0 was found using the area below the TSL. Procedure for the exponential traction separation law implemented in Warp3D was very similar. Obtained cohesive parameters were used in FEM computation for 3PB test. F-alloy modelling can be seen in Figure 4. J-integral in Warp3D is continually computed ahead the crack tip and his positions are changing during the element killing. Thereafter the construction of the $J-R$ curve can by constructed very precisely.

According the experimental observation the $J-R$ curve reflects various types of microstructures. The flat curves represents the duplex microstructure, rapidly increasing curves the lamelar microstructure and the curve between the nearly lamelar microstructure. In the following Figure 5 and Figure 6 one can see the influence of the notch shape on the microstructure damage processes.

C. Long fibre composites

The failure of composites has been investigated extensively from the micromechanical point of view. When a crack propagates in a composite material in a direction perpendicular to that of reinforced fibres, the failure process typically involves four basic mechanisms: matrix cracking, fibre/matrix debonding, fibre breakage and fibre pull-out. Critical problems in application of these materials are the interfaces between matrix and reinforcing fibres. The interface is very strip area with primary key property including the fracture toughness,
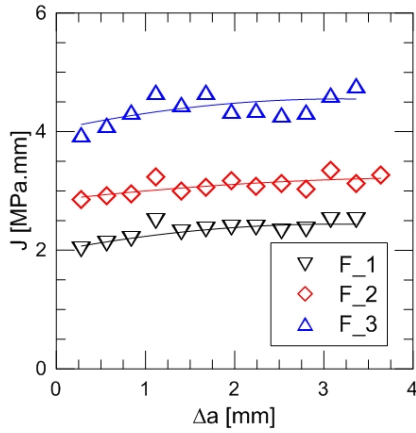
Fig. 6. $J - R$ curve: $K = 14$ MPa.m$^{1/2}$, $K = 16,3$ MPa.m$^{1/2}$, $K = 20$ MPa.m$^{1/2}$ (sharp notch, $\sigma_y = 300$ MPa).

Fig. 7. Traction separation (bridging) law modification.

strength and fracture behaviour. This interface plays the crucial role in stress transferring between reinforcement and matrix and so it determines the mechanical and fracture behaviour. The separation is given by the common influence between normal and tangential directions at the interface. Compound materials consist of two or more constituents with different properties complementing other. The degrading properties of one constituent are leveled off by better properties of the others. Damage evolution is sensitive to morphological parameters of the microstructure such as volume fraction, size and spatial distribution of reinforcements, interfacial strength and size defect.

For glass fibre composites, the interfacial properties are controlled by the sizing, which is applied to the glass fibres during manufacture. The change of sizing results in changes of these properties. This leads to the influence to the mechanical properties such as strength and fracture toughness. The concept of strength is used for characterizing crack initiation in composite design, while fracture toughness determines crack growth and damage development. Bridging occurs during cracking in mode I crack growth along the fibre direction. This failure mode plays an important role during delamination of fibre composites and cracks splitting around holes and notches. The fibre bridging zone must be modelled as a discrete mechanism on its own; failure is not just controlled by the cracking at the crack tip. The failure process can be described by a bridging law, which describes the relationship between the crack opening displacement and the local bridging tractions resulting from the bridging ligaments. This paper derives the necessary basics and equations to implement these laws into the commercial finite element code Abaqus with a cohesive user element. Different numerical adjustments of the bridging law will be discussed in detail in oral presentation. Crack aspects, such as crack opening shape and the influence of bridging law parameters, are studied based on the numerical results.

Now consider the specimen having a crack with bridging fibres across the crack faces near the tip. The bridging law is then taken to be identical at each point along the bridging zone. Since fibres will fail when loaded sufficiently, we assume the
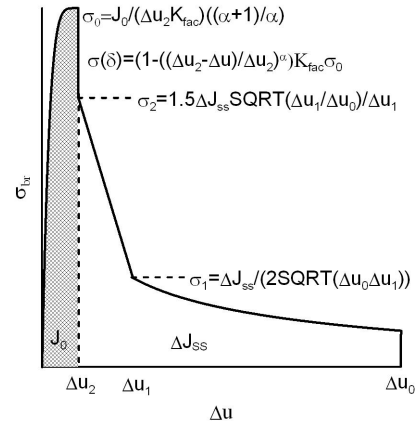
existence of a characteristic crack opening δ_0, beyond which the closure traction vanishes. Shrinking the path of the J-integral to the crack faces and around the crack tip gives

$$J = \int_0^{\delta^*} \sigma(\delta)\,\mathrm{d}\delta + J_{TIP} \qquad (7)$$

where J_{TIP} is the J-integral evaluated around the crack tip (during cracking is equal to the fracture energy of the tip, J_0). The integral is the energy dissipation in the bridging zone and δ^* is the end-opening of the bridging zone at the notch root. The bridging law can be determined by differentiating Eq. 7:

$$\sigma(\delta^*) = \frac{\partial J_R}{\partial \delta^*} \qquad (8)$$

where J_R is the value of J during crack growth. Initially, the crack is unbridged. Thus in Eq. 8 crack growth initiates when $J_R = J_{TIP} = J_0$. As the crack grows, J_R increases in accordance with Eq. 7. When the end opening of the bridging zone δ^* reaches δ_0, the overall R-curve attains its steady state value J_{ss}.

There are a variety of possible methods for implementing cohesive laws within commercial finite element programs. The most versatile is the development and programming of cohesive elements. These elements are in most cases defined with zero thickness and prescribe stresses based on the relative displacement of the nodes of the element. Similar work has also been undertaken with spring elements (force-opening relation), although in this case there might be simplifications required when calculating the equivalent nodal spring forces from the surrounding elements. The procedure is not straight forward when springs are connected to elements with non-linear shape functions, such as 8-node elements.

The constitutive expression can be expressed either with a linear displacement term for Δu, or with a coupled form, where Δu is included with non-linear dependence. The preferred option depends on the form of the constitutive equation Eq. 7 and its numerical implementation:

$$J_R(\delta^*) = J_0 + \Delta J_{SS}\left(\frac{\delta^*}{\delta_0}\right)^{1/2}. \qquad (9)$$

Two points need to be addressed during the numerical adjustment: removal of the stress singularity at $\Delta u = 0$ and
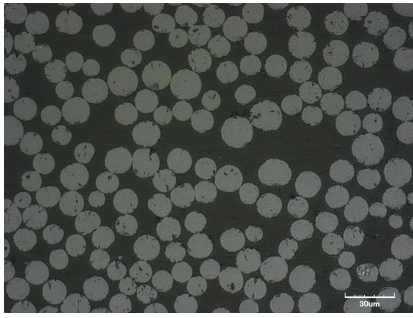
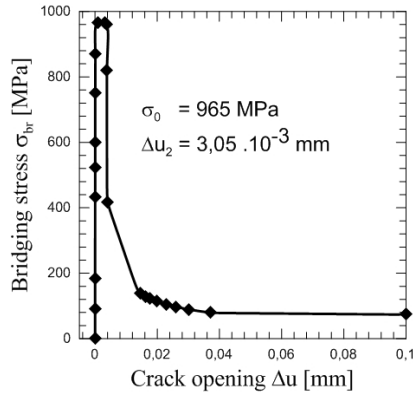Fig. 8.   Image of the microstructure.

Fig. 9.   Traction separation law after calibration procedure.

incorporation of the initial fracture strength J_0 improved traction separation law as can be seen in Figure 7. The material used for the bridging stresses modelling was a commercially available SiC Nicalon fibre reinforced borosilicate glass matrix composite (see Figure 8). Properties of the glass matrix, SiC fibres and composite were: Young modulus 63, 198, 118 GPa, Poisson ratio 0.22, 0.20, 0.21, tensile strength 60, 2750, 600-700 MPa.

For the crack growth modelling the following data determined experimentally were used: $J_0 = 6200$ J/m^2, $J_{ss} = 18500$ J/m^2, $\Delta u_c = 0.1$ mm, $\Delta u_1 = 0.013$ mm. Calibrated data and the final shape of the bridging law can be seen on the following Figure 9.

D. Ceramics

Ceramics such as silicon nitride (Si3N4) are acknowledged as the first choice for modern bearing applications. However, in addition to severe working conditions such as high temperatures and corrosive environments, rolling where elements are subjected to high cyclic contact stresses during service [1]. It is well recognized that the properties of ceramics can be profoundly enhanced by suitably tailoring the microstructure based on realistic application and working conditions. Namely, the effects of tailoring the grain structure on the fracture toughness of silicon nitride were demonstrated in [2]. Similarly, the influence of boundary phase manipulation and the effect of grain bridging on the strength and toughness were illustrated in [3]. In order to improve the lifetime of ceramic components and realize cost and energy efficient

manufacturing processes, two main issues have to be addressed: i) materials with increased functionality and optimum properties should be fabricated and tailored for a wide diversity of requirements (materials design and optimisation); ii) the progress of degradation processes should be predicted and evaluated (damage analysis), focusing in particular on damage mechanisms occurring under realistic working and loading conditions. his knowledge leads to the design of materials with superior performance in machine components.

Two directions were investigated (in the pressing direction and perpendicular to this direction). The level of anisotropy in elastic modulus values is relatively low: around 1 GPa, i. e. $E_A = 293.07$ GPa and $E_B = 293.83$ GPa; Poisson ratio has been determined to be 0.283.

The extended finite element method (XFEM) was first introduced by [34]. It is an extension of the conventional finite element method based on the conception of partition of unity by [35]. The presence of discontinuities is ensured by special enriched function. For purpose of fracture analysis, the enrichment function typically consist of the near tip asymptotic functions that captures singularity around the crack tip and the discontinuous function that represents the jump in displacements across the crack tip surfaces. The approximation for displacement vector function u with the partition of unity enrichment is

$$u_{XFEM} = \sum_{i \in I} N_i(x)u_i + \sum_{i \in J} N_i(x)H(x)a_i \qquad (10)$$
$$+ \sum_{i \in K} \left[N_i(x) \sum_{\alpha=1}^{4} F_\alpha(x)b_{i\alpha} \right]$$

where $N_i(x)$ are the usual nodal shape functions; u_i is nodal displacement vector associated with the continuous part of the finite element solution, the second term is product of the nodal enriched degree of freedom vector a_i, and associated with discontinuous jump function $H(x)$ across the crack surfaces, the third term is the product of the nodal enriched degree of the freedom vector $b_{i\alpha}$ and associated elastic asymptotic crack tip function, F_α (x).

The formulae and laws that govern the behaviour of the XFEM cohesive segments for crack propagation are very similar to those used for cohesive elements with traction separation law. The similarities extend to the linear elastic traction separation model, damage initiation criteria and similar damage evaluation law. Input parameters used for modelling using Abaqus are: the maximum principal stress criterion 1000 MPa, damage evolution $K = 5.3$ MPa.m$^{1/2}$, Young modulus 293 000 MPa, Poisson ratio 0.283.

Saturation in the $J - R$ curve has been reached for XFEM modelling substantially later than for the cohesive zone approach. Usually the crack length was greater than 20 μm. This observation is predicable because the XFEM model is not incorporating the bridging mechanism into the cohesive law. The expected behaviour of the $J - R$ curve based on the literature data should be different and the saturation is expected for the crack lengths in the interval of 10-15 μm. The discrepancy comparing literature with our results can be seen in the different microstructure and / or due to numerical
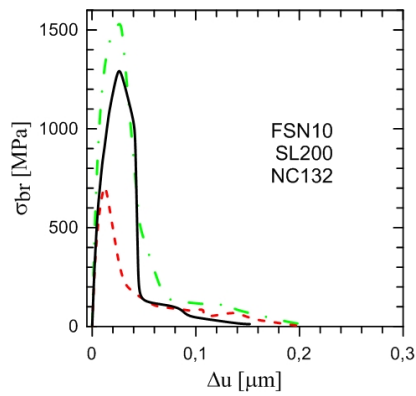
Fig. 10. Bridging law after calibration procedure.
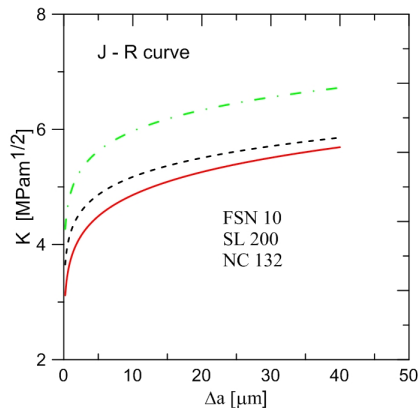

Fig. 11. J-R curve prediction.

oscillation which can lead to the underestimation of K-values.

IV. Conclusion

The cohesive zone modelling has the capacity to investigate the interplay between the local microstructure and the various material properties (mainly fracture toughness). The shape of the $J - R$ curve is more determined by the material curve than by the shape of the traction separation law and reflects the material microstructure. Knowledge and practice experiences
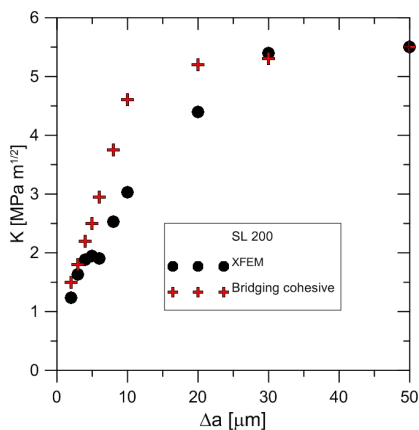

Fig. 12. J-R curve prediction for XFEM and cohesive modelling.

how to use cohesive elements for the ductile and brittle fracture has been obtained and the crack growth modelling for heterogeneous materials has been tested too. Modelling has been confronted with the classical fracture mechanics concepts. Increased attention has been applied to intermetallics and to the influence of the microstructure on the fracture process. To determine the basic material characteristics of intermetallic alloys is not the standard thing. Therefore for the numerical modelling the parametric approach has been applied to find the connection between fracture micromechanisms and input data. Obtained results and running analysis of the microstructure will enable to concentrate our future work for crack prediction in dimension close to grain size.

For fibre composites in mode I crack growth in unidirectional fibre composites is modelled; fibre cross-over bridging occurs during cracking along the fibre direction. Crack-bridging mechanisms can provide substantial increases in the toughness coupled with the strength in ceramics and saturation in the $J - R$ curve has been reached for XFEM modelling substantially later than for the cohesive zone approach.

References

[1] G. I. Barenblatt, The formation of equilibrium cracks during brittle fracture. *PMM (Prikladnaya Matematika i Mekhanika)* 3 (1959), 434–444.

[2] D. S. Dugdale, Yielding of steel sheets containing slits. *Journal of the Mechanics and Physics of Solids* 8 (1960), 100–104.

[3] C. Shet and N. Chandra, Analysis of energy balance when using cohesive zone models to simulate fracture process. *ASME Journal of Engineering Materials and Technology* 124 (2002), 440–450.

[4] H. Li and N. Chandra, Analysis of crack growth and crack-tip plasticity in ductile materials using cohesive zone models. *International Journal of Plasticity* 19 (2003), 849–882.

[5] J. Planas, M. Elices, G. V. Guinea, F. J. Gómez, D. A. Cendón and I. Arbilla, Generalizations and specializations of cohesive crack models. *Engineering Fracture Mechanics* 70 (2003), 1759-1776.

[6] K. Park and G. H. Paulino, Cohesive zone models: A critical review of traction-separation relationships across fracture surfaces. *Applied Mechanics Reviews* 64 (2011), 060802: 1–20.

[7] N. Moës and T. Belytschko, Extended finite element method for cohesive crack growth, *Engineering Fracture Mechanics* 69 (2002), 813-833.

[8] S. Li and S. Ghosh, Multiple cohesive crack growth in brittle materials by the extended Voronoi cell finite element model, *International Journal of Fracture* 141 (2006), 373-393.

[9] J. J. C. Remmers, R. de Borst and A. Needleman, The simulation of dynamic crack propagation using the cohesive segments method. *Journal of the Mechanics and Physics of Solids* 56 (2008), 70-92.

[10] P. A. Klein, J. W. Foulk, E. P. Chen, S. A. Wimmer and H. J. Gao, Physics-based modelling of brittle fracture: cohesive formulations and the application of meshfree methods. *Theoretical and Applied Fracture Mechanics* 37 (2001), 99–166.

[11] F. Barra, A. Levermann and I. Procaccia, Quasistatic brittle fracture in inhomogeneous media and iterated conformal maps: modes I, II, and III. *Physical review E* 66 (2002), 066122: 1–16.

[12] P. Gumbsch, Modelling brittle and semi-brittle fracture processes. *Materials Science and Engineering A* 319-321 (2001), 1-7.

[13] B. Chong, Simulation of crack growth using cohesive crack method. *KSCE Journal of Civil Engineering* 14 (2010), 765–772.

[14] P. B. Warren, Fracture of brittle materials: effects of test method and threshold stress on the Weibull modulus. *Journal of the European Ceramic Society* 21 (2001), 335–342.

[15] R. Danzer, P. Supancic, J. Pascual and T. Lube, Fracture statistics of ceramics Weibull statistics and deviations from Weibull statistics. *Engineering Fracture Mechanics* 74 (2007), 2919-2932.

[16] L. B. Freund, Brittle crack growth modeled as the forced separation of chemical bonds within a *K*-field. *Journal of the Mechanics and Physics of Solids* 64 (2014), 212-222.

[17] Z. Shabir, E. Van der Giessen, C. A. Duarte and A. Simone, The role of cohesive properties on intergranular crack propagation in brittle polycrystals. *Modelling and Simulation in Materials Science and Engineering* 19 (2011), 035006: 1–21.

[18] G. Hütter, T. Linse, S. Roth, U. Mülich and M. Kuna, A modeling approach for the complete ductile-brittle transition region: cohesive zone in combination with a non-local Gurson-model, *International Journal of Fracture* 185 (2014), 129–153.

[19] A. Yavari, Generalization of Barenblatt's cohesive fracture theory for fractal cracks. *Fractals-Complex Geometry Patterns and Scaling in Nature and Society* 10 (2002), 189–198.

[20] A. Carpinteri, B. Chiaia and P. Cornetti, A mesoscopic theory of damage and fracture in heterogeneous materials. *Theoretical and Applied Fracture Mechanics* 41 (2004), 43-50.

[21] M. P. Wnuk and A. Yavari, A discrete cohesive model for fractal cracks. *Engineering Fracture Mechanics* 76 (2009), 548-559.

[22] M. Davydova and S. Uvarov, Fractal statistics of brittle fragmentation. *Frattura ed Integrità Strutturale* 24 (2013), 60–68.

[23] G. Del Piero and D. R. Owen, Structured deformations of continua. *Archive for Rational Mechanics and Analysis* 124 (1993), 99–155.

[24] M. arc Frančis and G. Royer-Carfagni, Structured deformation of damaged continua with cohesive-frictional sliding rough fractures. *European Journal of Mechanics / A Solids* 24 (2005), 644-660.

[25] D. H. Allen and Ch. R. Searcy, A micromechanical model for a viscoelastic cohesive zone. *International Journal of Fracture* 107 (2001), 159-176.

[26] S. Li and G. Wang, On damage theory of a cohesive medium, *International Journal of Engineering Science* 42 (2004) 861885

[27] C. V. Verhoosel1, J. J. C. Remmers, M. A. Gutiérrez and R. de Borst, Computational homogenisation for adhesive and cohesive failure in quasi-brittle solids. *International Journal for Numerical Methods in Engineering* 83 (2010), 1155-1179.

[28] S. May, J. Vignollet, and R. de Borst, A numerical assessment of phase-field models for brittle and cohesive fracture: Γ-convergence and stress oscillations. *European Journal of Mechanics / A Solids*, to appear (2015), 27 pp. (doi: 10.1016/j.euromechsol.2015.02.002).

[29] E. Reyes, M. J. Casati and J. C. Gálvez, Cohesive crack model for mixed mode fracture of brick masonry. *International Journal of Fracture* 151 (2008), 29–55.

[30] G. Alfano, S. Marfia and E. Sacco, A cohesive damagefriction interface model accounting for water pressure on crack propagation. Computer Methods in Applied Mechanics and Engineering 196 (2006), 192-209.

[31] J. Zhang, Ch. K. Y. Leung and Y. Gao, Simulation of crack propagation of fiber reinforced cementitious composite under direct tension. *Engineering Fracture Mechanics* 78 (2011), 2439-2454.

[32] A. Karamnejad, V. P. Nguyen and L. J. Sluys, A rate-dependent multi-scale crack model for concrete. VIII International Conference on Fracture Mechanics of Concrete and Concrete Structures *Proceedings of FraMCoS-8 (8th International Conference on Fracture Mechanics of Concrete and Concrete Structures)* in Toledo (2013), 48: 1–11.

[33] H. Zhang and D. Wei, Fracture and damage behaviors of concrete in the fractal space. *Journal of Modern Physics* 1 (2010), 48–58.

[34] T. Belytschko and T. Black, Elastic crack growth in finite element with minimal remeshing. *International Journal of Numerical Methods in Engineering* 46 (1999), 601–620.

[35] I. Babuška and U. Banerjee, Stable generalized finite element method (SGFEM). *Computer Methods in Applied Mechanics and Engineering* 201 (2012), 91–111.

[36] M. Lengauer and R. Danzer, Silicon nitride tools for the hot rolling of high-alloyed steel and superalloy wires - crack growth and lifetime prediction. *Journal of the European Ceramic Society* 28 (2008), 2289-2298.

Jiří Vala (*1956) is professor at the Brno University of Technology, Faculty of Civil Engineering, Czech Republic, 602 00 Brno, Veveří 95, e-mail *vala.j@fce.vutbr.cz.*

Vladislav Kozák (*1954) is researcher at the Institute of Physics of Materials in Brno, Academy of Sciences of the Czech Republic, 616 62 Brno, Žižkova 22, e-mail *kozak@ipm.cz.*